EMULATE Deliverable D7: Assessment of the variability of the observed North Atlantic and European atmospheric circulation for the last 150 years in relation to SST patterns.

Hadley Centre (Partner 2), UBERN (partner 6) and UA (partner 3).

Chris Folland[1], Adam Scaife[1], David Fereday[1], Jeff Knight[1], Thomas Toniazzo[1], Jucundus Jacobeit[2], Andreas Philipp[2] and Paul Della-Marta[3].

[1]- Hadley Centre, Met Office, UK.
[2]- University of Augsburg, Germany.
[3]- University of Bern, Switzerland.

1. Introduction

European climate is thought to be influenced by variations in ocean surface conditions occurring on interannual and longer timescales and these links offer the potential for predictability at longer lead time than is offered by conventional weather forecasting. The relative importance of the ocean in determining atmospheric variability is also thought to increase at multiannual and longer timescales. In addition, the ocean also responds to the atmospheric state, integrating high frequency atmospheric anomalies due to its large thermal inertia and relatively long circulation timescales. This creates the potential for feedbacks on longer timescales than occur in the atmosphere alone and gives rise to important coupled ocean-atmosphere modes of variability, especially in the tropics, such as the El Niño Southern Oscillation (ENSO). The role of the oceans in determining extratropical atmospheric variability is less clear and effects on the Atlantic and Europe region are therefore one focus of the EMULATE project.

We describe results for prominent climate modes of variability and from a variety of analysis methods ranging from composite analysis to canonical correlation analysis, to the application of a new form of clustering technique to atmospheric data. The clustering algorithm developed in WP2 has been applied to the EMULATE mean sea level pressure data set to analyse possible links with sea-surface temperature (SST). The clustering algorithm is carried out in the full pressure space of the EMULATE data and uses each gridpoint independently.

Simulated annealing clustering is a variant of conventional k-means cluster analysis, but differs in two points:

i) There is no starting partition needed (i.e. it starts on a randomized starting partition respectively).

ii) During the process of rearrangements of objects between clusters, temporary worsening of the partition between clusters is allowed.

The latter is included to avoid potential local but non-optimal minima of the optimisation function which is impossible for conventional k-means optimisation algorithms. Simulated annealing is therefore superior to all other clustering techniques under consideration (see WP2) when comparing strategies to reach the best partitioning of a certain dataset. One drawback of this technique is that it necessarily includes some randomness and its results may also therefore be dependent on the random choices made to carry out the simulated annealing (although to a much lesser extent than with all other techniques). The simulated annealing clustering technique minimizes the influence of this randomness by running simulated annealing clustering analysis repeatedly, each time with a changing series of random numbers and selecting the result converging nearest to the global minimum of the optimisation function, i.e. the best result available. This ensures a very stable solution for the optimisation problem and avoids convergence on local optima of low quality. A full description of the technique is given in WP2.

In order to examine the interactions of the atmospheric circulation patterns with SSTs, the classification of daily MSLP fields generated by the clustering algorithm is used to form composite SST anomaly fields associated with occurrences of each cluster. The year is divided into six 'natural' seasons of two months each (JF, MA, MJ, JA, SO, ND) and the daily MSLP fields for each season are clustered separately. The MSLP field for each day of each season is classified as belonging uniquely to a particular cluster for that season. The composite SST anomaly fields are generated as a weighted average of the deseasonalised monthly mean SST fields from the HadISST (v1.1) dataset, available from 1870 onwards. The HadISST data is high pass filtered (using a half power of 10 years). Only high pass results are discussed here.

2) The winter North Atlantic Oscillation (NAO)

Surface Pressure

The winter NAO is the primary mode of variability over the North Atlantic region on timescales from days to multi-decades. The basic pattern of a meridional dipole with centres of action near Iceland and the Azores is easily captured by the EMULATE cluster analysis (Fig.1).

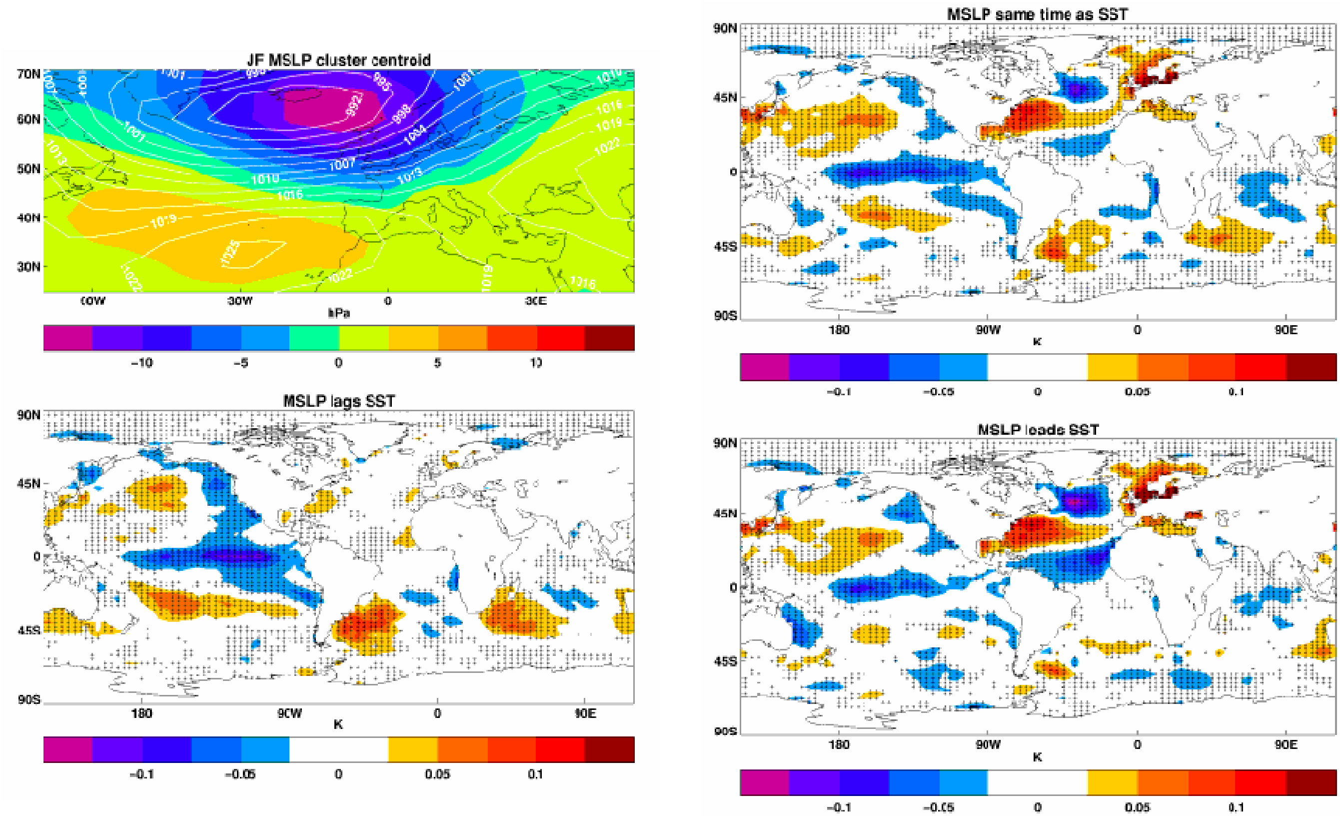

Figure 1. Centroid of the EMSLP cluster best representing the winter NAO for JF (upper left). Simultaneous SST anomalies (upper right) and associated SST anomalies at positive and negative lags (lower left and lower right respectively). Significant gridpoints at the 5% level of confidence are marked with a cross and are calculated by a Monte-Carlo technique using similar, randomly generated SST composites.

Simultaneous SST anomalies show a tripole structure in North Atlantic SST with warm mid-latitude SSTs and cooler SSTs to the North and South being associated with positive NAO anomalies as found in several other studies (e.g. Rodwell et al. 1999). A stronger signal with a similar pattern is found in the Atlantic SST following positive NAO circulation anomalies, leading to the possibility of positive feedback (Frankignoul, 1985). Although we find little indication of SST forcing the NAO in the months immediately prior to the occurrence of atmospheric anomalies, there is an apparent connection between positive NAO weather patterns and the SST distribution in the previous spring:

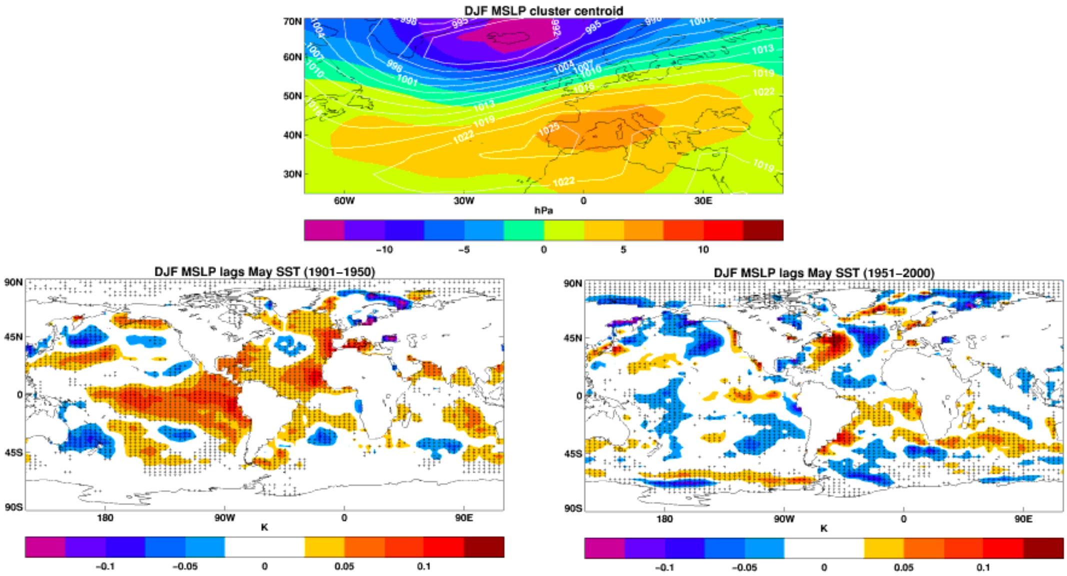

Figure 2. Centroid of the EMSLP cluster best representing the positive phase of the winter NAO for DJF (upper). Corresponding SST composite fields at positive and negative lag for the periods 1901-1950 and 1951-2000 (lower left and lower right). Significant gridpoints at the 5% level of confidence are marked with a cross and are calculated by a Monte-Carlo technique using similar, randomly generated SST composites.

Fig.2 illustrates this connection using composite SST fields for the May preceding each DJF season when the NAO anomalies occurred. The SST composite exhibits a statistically significant North Atlantic SST tripole pattern in the 1951-2000 composite but not in the 1901-1950 composite. This is consistent with the results of Rodwell and Folland (2002, 2003) and suggests that May SST patterns may contain some predictability of the frequency of positive NAO weather patterns in the following winter. This result supports the soundness of a seasonal forecasting technique for the winter NAO based on the previous May SST in the North Atlantic that is already operational.

Temperature

The simultaneous relationship between the extended winter season (DJFM) SST and European land surface air temperature (ET) has also been explored using a Canonical Correlation Analysis (CCA) in the Empirical Orthogonal Functions (EOF) space. It has been found that there is a strong connection between the two datasets. Monthly winter SST explains around 37% of monthly winter ET variability (Fig. 3). The characteristic tripole SST pattern is found to be the most important mode of SST variability that is connected with a large monopole of anomalous ET over Europe.

Composite analysis of extreme ET winters are shown in figure 4. In this study, the selection of the extreme winters was based on the first canonical score. Extreme warm and cold winters’ CCA1 scores exceed +1 and -1.5 standard deviations, respectively. Figure 4 shows that that cold (warm) European winters are associated with cooler (warmer) than normal simultaneous SSTs around Europe and weak (strong) NAO.

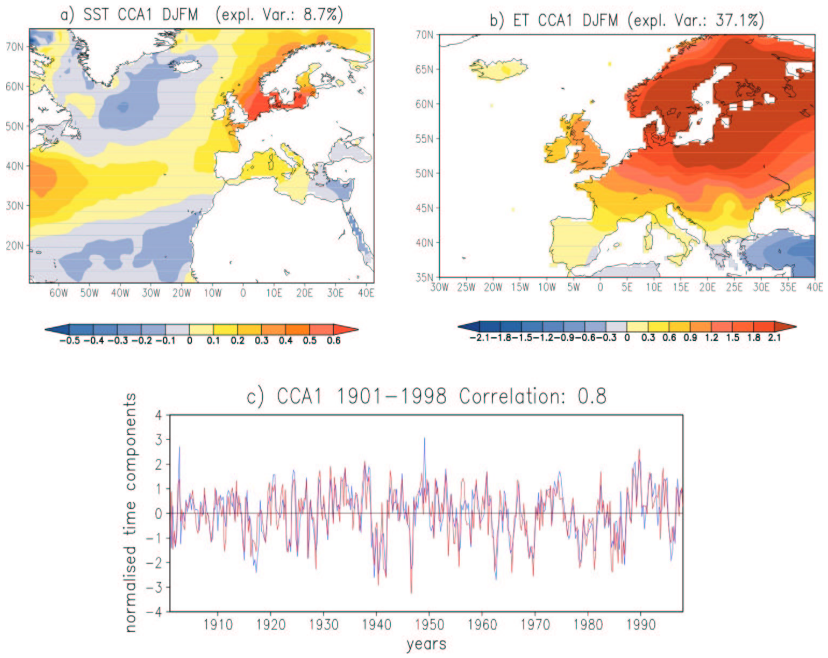

Figure 3. First CCA pattern of (a) SST and (b) ET in (both in °C), and corresponding scores (c) for extended winter (DJFM) 1901-1998. The blue line in (c) is the SST, the red line the ET.

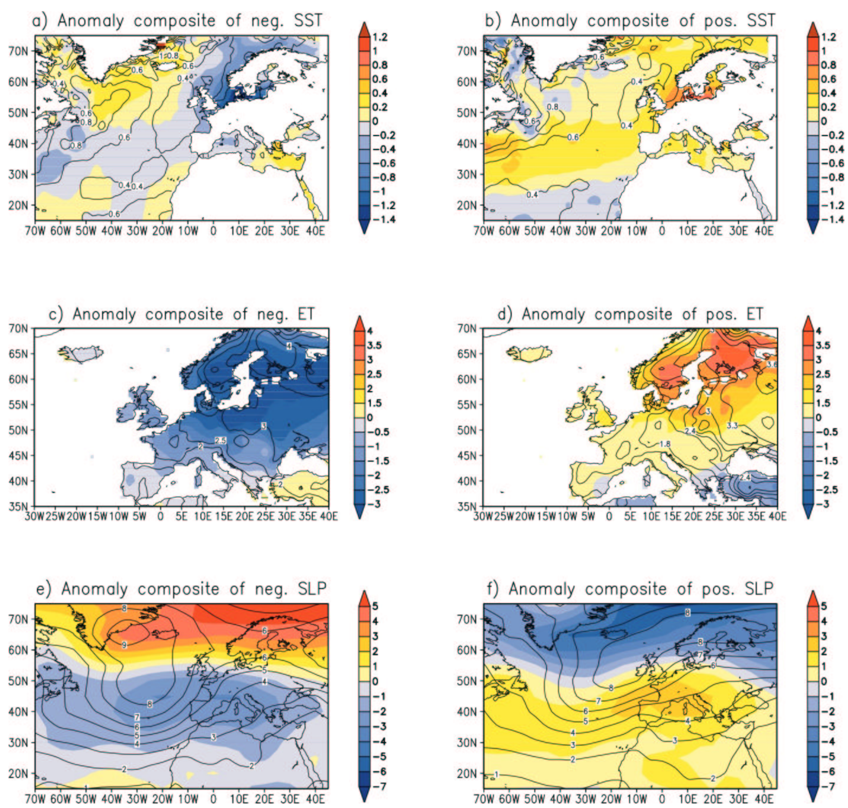

Figure 4. a) SST anomaly composite of exceptional negative ET, b) SST anomaly composite of exceptional positive ET, c) anomaly composite of exceptional negative ET, d) anomaly composite of exceptional positive ET, e) SLP anomaly composite related to exceptional negative ET, f) SLP

anomaly composite of exceptional positive ET. Black contours are standard deviations.

Precipitation

Exploratory studies have also been conducted on the relationship between Atlantic SSTs and European winter precipitation (EP) for the twentieth century. Again, the extended winter season has been used, however the EOF/CCA analyses are based on seasonally averaged SST and EP. Figure 5 presents the first canonical pair between the winter Atlantic SSTs and European precipitation.

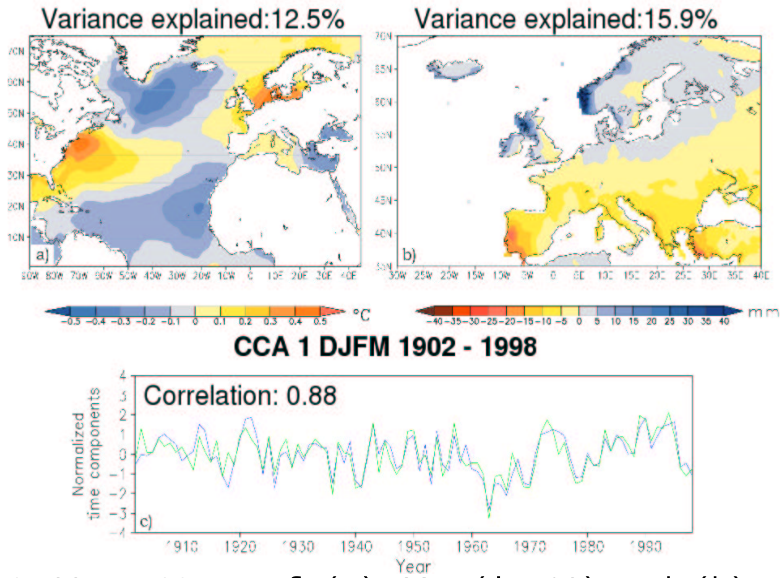

Figure 5. First CCA pattern of (a) SST (in °C) and (b) EP (in mm), and corresponding scores (c) for extended winter average (DJFM) 1901-1998. The blue line is the SST, the green line the EP.

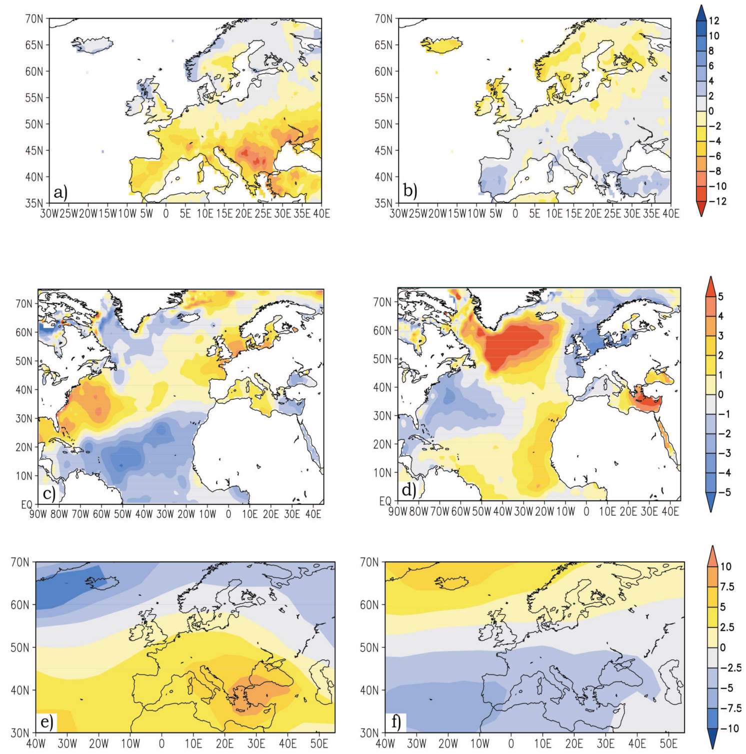

Figure 6. a) anomaly composite of exceptional negative EP, b) anomaly composite of exceptional positive EP, c) SST anomaly composite of

exceptional negative EP, d) SST anomaly composite of exceptional EP, e) SLP anomaly composite related to exceptional negative EP, f) SLP anomaly composite of exceptional positive EP.

In the positive mode (positive CCA scores in Fig. 5c) positive SST anomalies around the European coasts, the North Sea and along the US east coast and negative anomalies in the subtropics and around Greenland are connected with below normal precipitation south of around 50°N and wetter conditions over Northern Europe.

Composite analysis of extreme EP winters are shown in figure 6. Extreme warm and cold winters' CCA1 scores exceed +1 and -1 standard deviations, respectively. Wet winters with wet conditions in northern Europe and dry conditions in central and southern Europe are associated with warmer than normal SSTs around Europe and the east coast of North America and positive NAO.

3) The Summer North Atlantic Oscillation

The summer North Atlantic Oscillation is the summer analogue of the better known winter North Atlantic Oscillation. Both phenomena can be defined by the first empirical orthogonal function of extratropical North Atlantic sea level pressure in their respective seasons. Fig. 7 shows the North Atlantic Oscillation pattern in all four three month seasons (Hurrell et al, 2003) using the Trenberth and Paolino (1980) sea level pressure data set.

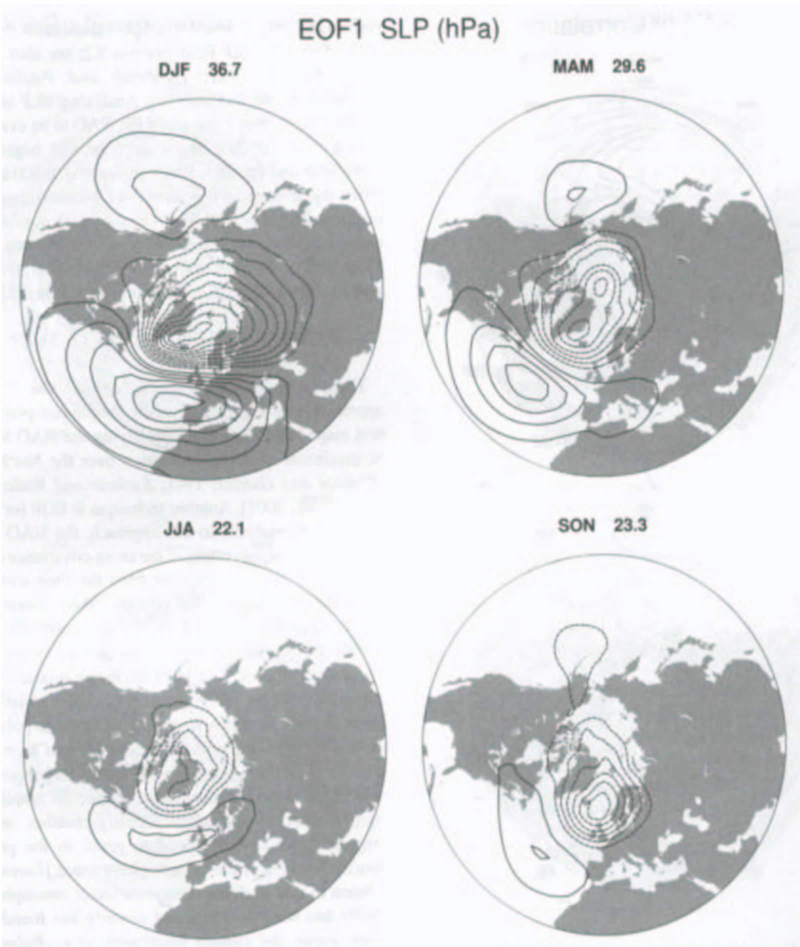

Figure 7. The annual cycle of the North Atlantic Oscillation as defined by the first covariance empirical orthogonal function of sea level pressure over the region 20°-70°N, 90°W-40°E. Also shown is the percentage

of total variance explained, 1899-2001, based on the Trenberth and Paolino monthly surface pressure data set. Patterns are in hPa obtained by regressing the hemispheric sea level pressure anomalies on the EOF1 time series. Contour increments 0.5hPa with no zero contour.

In this note we concentrate on the *high* summer period July and August when temporal variations of the summer NAO are most coherent. An initial discussion of the summer NAO phenomenon can be found in Hurrell and Folland (2002).

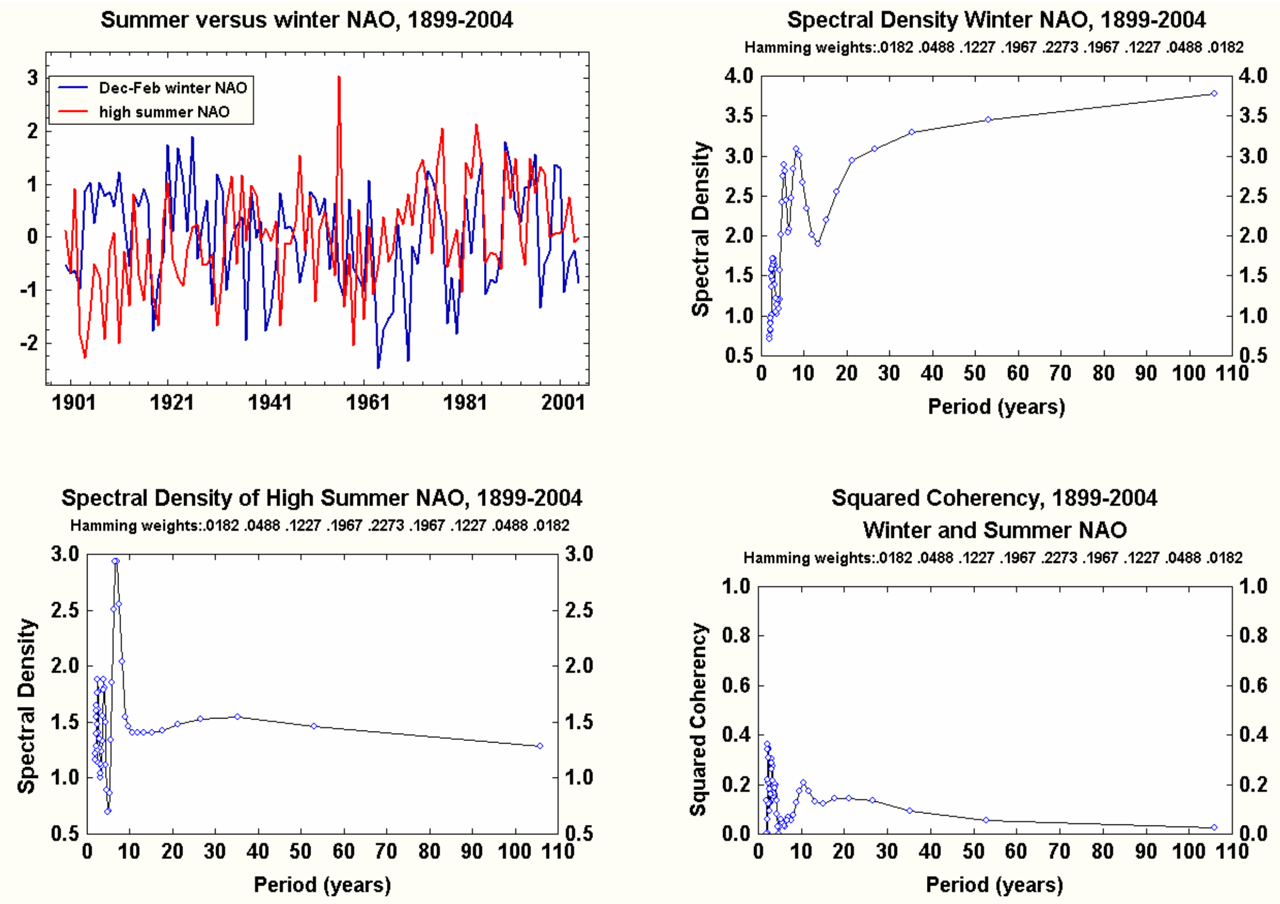

Figure 8a-d. Comparison of the winter and summer NAO. Time series in Fig. 8a is standardised over the period 1899-2004. Spectra are smoothed used a hamming filter with weights as shown. The coherence squared significance estimates allow for filtering.

Fig. 8a shows standardised time series of the high summer NAO since 1899, based on the above EOF analysis, compared to the winter NAO based on an index of the difference in surface pressure between the Azores and Iceland for 1899-2004. The correlation between the summer and winter NAO time series over 1899-2004 is only 0.05. Over the period 1950-2004 the correlation rises a little to 0.27 but is still not significant. Figs 8b and 8c and the squared coherence between the spectra (Fig 8d) indicate that the spectra have relatively little in common over 1899-2004, though a peak near 7-8 years is seen in both summer and winter. In high summer, this peak is relatively rather stronger and worthy of investigation. However the squared coherence between the high summer and winter NAO (which can be thought of as their squared correlation at each period) does not approach the 5% confidence level of 0.52 at any period. So the summer and winter NAOs, as defined here, can be regarded as effectively independent in time over the 1899-2004 period.

The summer NAO also appears prominently in a cluster analysis of July and August sea level pressures (Fig. 9), based on the new daily EMULATE surface pressure data set, 1850-2003. The analysis shown here groups days into 6 high summer clusters. Fig. 9 shows the observed July – August clusters based on single day events. The two cluster patterns shown are very similar to EOF1 in Figure 7, for the area of overlap, but have opposite signs. Together these clusters consist of 30% of all days with nearly equal populations of the positive and negative patterns. The negative summer NAO anomaly tends to be a few hundred km to the west south west of the positive contours in the positive summer NAO cluster. Looking at the absolute pressure contours (white), it can be seen that the negative cluster corresponds to cyclonic flow over north west Europe, especially the UK, and the positive cluster to anticyclonic conditions, especially over the UK. So the changes represented by these two clusters are large compared to the variability of sea level pressure in high summer over the UK. Thus we may regard the summer NAO as a major feature of high summer North Atlantic and European climate variability in the same way as the winter NAO is a major feature of winter climate variability.

Figure 10, based on EOF1 for 1899-2004, shows that the summer NAO also has coherent multidecadal fluctuations. It tended to be negative on these time scales in the early part of the twentieth century, near neutral between about 1930 and 1955, negative in the following decade with a rather rapid increase peaking in the 1980s to positive decadal averages. There is some evidence since the late 1990s of a reduction to only a weakly positive summer NAO.

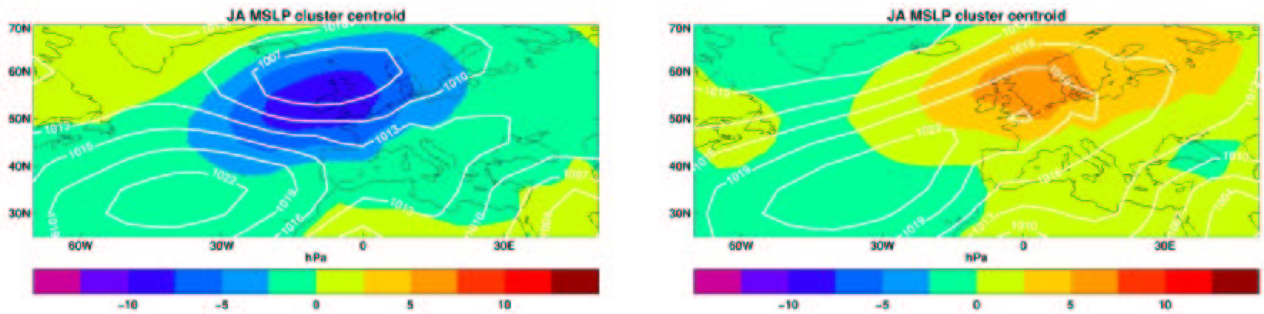

Figure 9. The two sea level pressure clusters that contribute to the summer NAO, based on individual days, 1850-2003. Absolute pressures are contoured white, anomalies from a 1961-90 average are coloured. 30% of all days are classified in both clusters, which are nearly equiprobable.

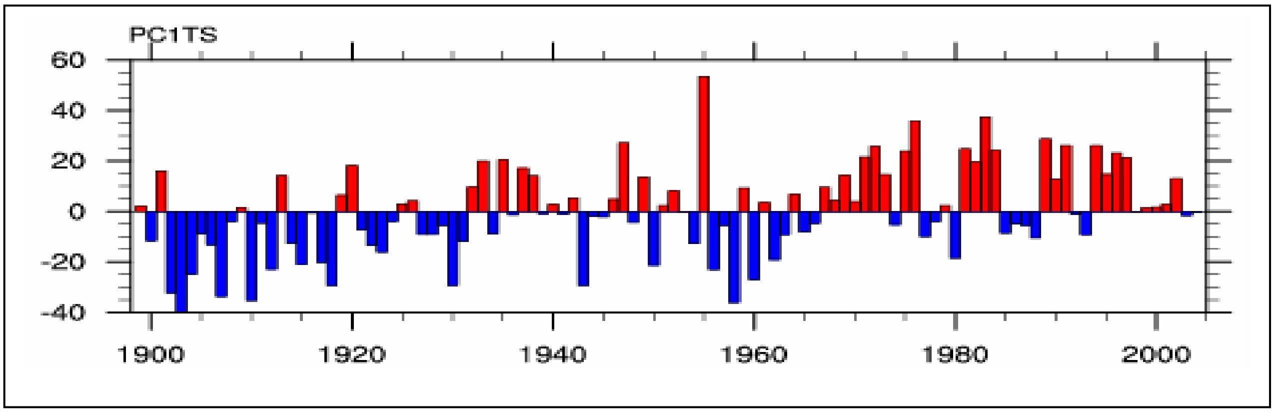

Figure 10. Time series of EOF1 in high summer, 1899-2004, using the Trenberth and Paolino sea level pressure data set.

The behaviour of the summer NAO is as marked in its own season as the decadal to interdecadal variations in the winter NAO, given the weaker variation of sea level pressure in high summer. To illustrate this, the impact of decadal summer NAO variations on sea level pressure and rainfall is illustrated in Fig 11. The summer NAO is associated with considerable multidecadal variations in atmospheric pressure and, not surprisingly, rainfall over the North Atlantic and European region (Figs 11a, 11b). The tendency to dry high summers in recent decades over the UK and a region extending towards western Russia is notable. Over the Mediterranean, summers have tended to become wetter. However, Fig. 10 indicates that this tendency has probably ceased and may have started to reverse.

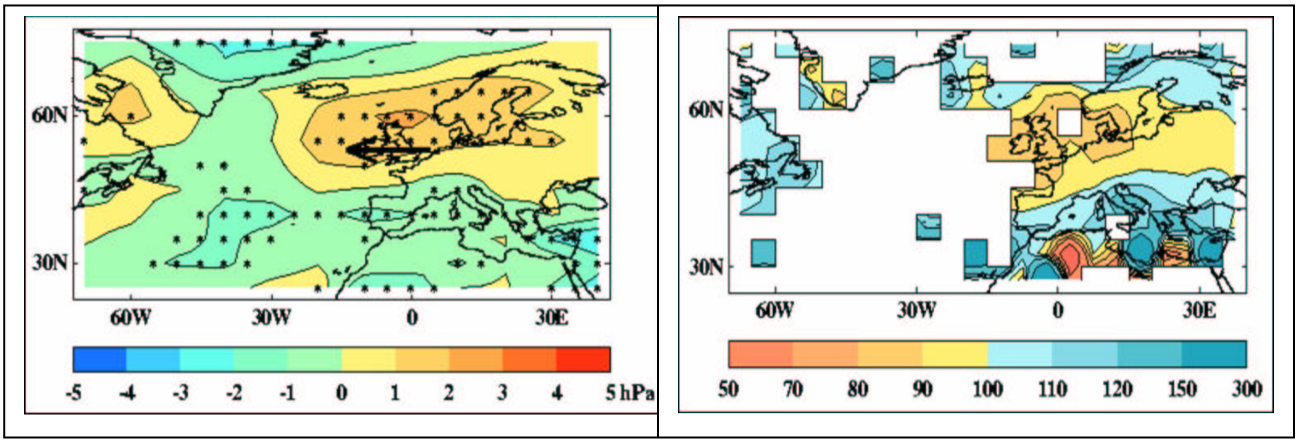

Figure 11. (a) Differences in sea level pressure between a period of high values of EOF1 (1967-1998) and relatively low values (1921-60) (b) Rainfall in 1967-1998 (based on the Hulme data set) as a percentage of the 1921-60 average. Stars in (a) show grid points where sea level pressure is significantly different between the two periods at the local 5% confidence limit. The area shown is clearly highly field significant.

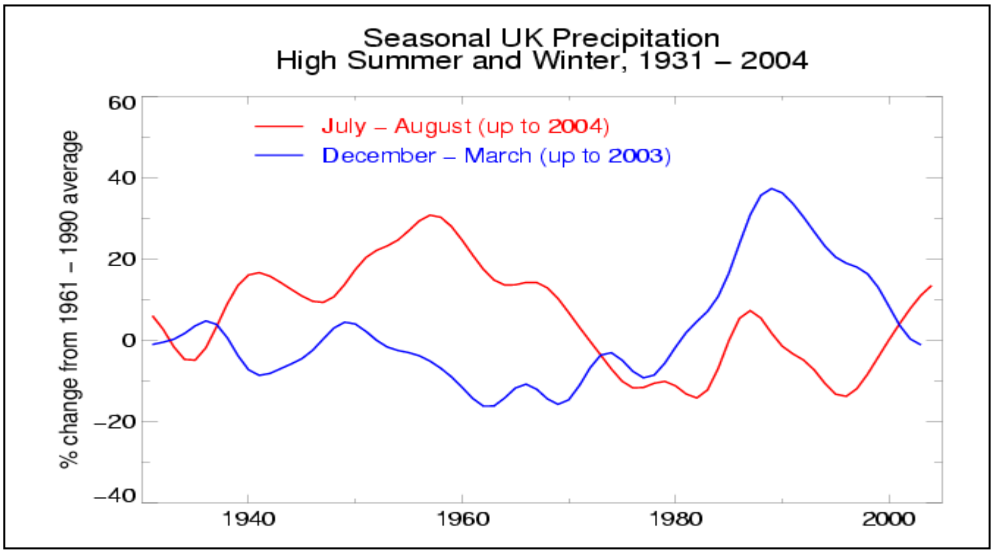

Figure 11c) Decadal variations of rainfall in South East England compared to those in North West Scotland, 1931-2004, based on regional UK rainfall series (Alexander and Jones, 2001).

Fig. 11c shows an approximately decadally averaged time series of rainfall, expressed as a percentage of the 1961-90 average, for south East England in high summer. This is a region very strongly affected by the summer NAO. For comparative purposes a comparable time series of rainfall in winter (December to March) is shown for North West Scotland (Fig. 11c); this is known to be strongly affected by the winter NAO (Fig. 5). Note that compared to the 1950s, south east England rainfall has averaged persistently 30% lower over the 20 years from the mid 1970s to the late 1990s, though with signs of a slight recovery to wetter conditions since then as might be expected from Fig. 10. These fluctuations, and the future course of high summer rainfall, are clearly of strong societal importance. It is interesting to note that the famous 1975/76 drought over UK, particularly severe in summer, fell at the beginning of the really dry recent decades. This drought was followed by a number of other drought summers including 1984 when the UK briefly appointed a Minister for Drought.

Figure 11d extends this analysis geographically using an NCAR rainfall data set. A feature indicated by Fig. 11d is a possible link between longer term variation in high summer rainfall related to the summer NAO (see Fig. 11a) and summer monsoon rainfall over North Africa, e.g. the Sahelian region of Africa. This link was first noticed by Folland et al (1988) in an early study before the summer NAO was named; the relationship has held up well since then (Fig. 12), suggesting a real relationship between Sahel rainfall and the summer NAO on decadal time scales. There is also some resemblance on subdecadal time scales which needs investigating.

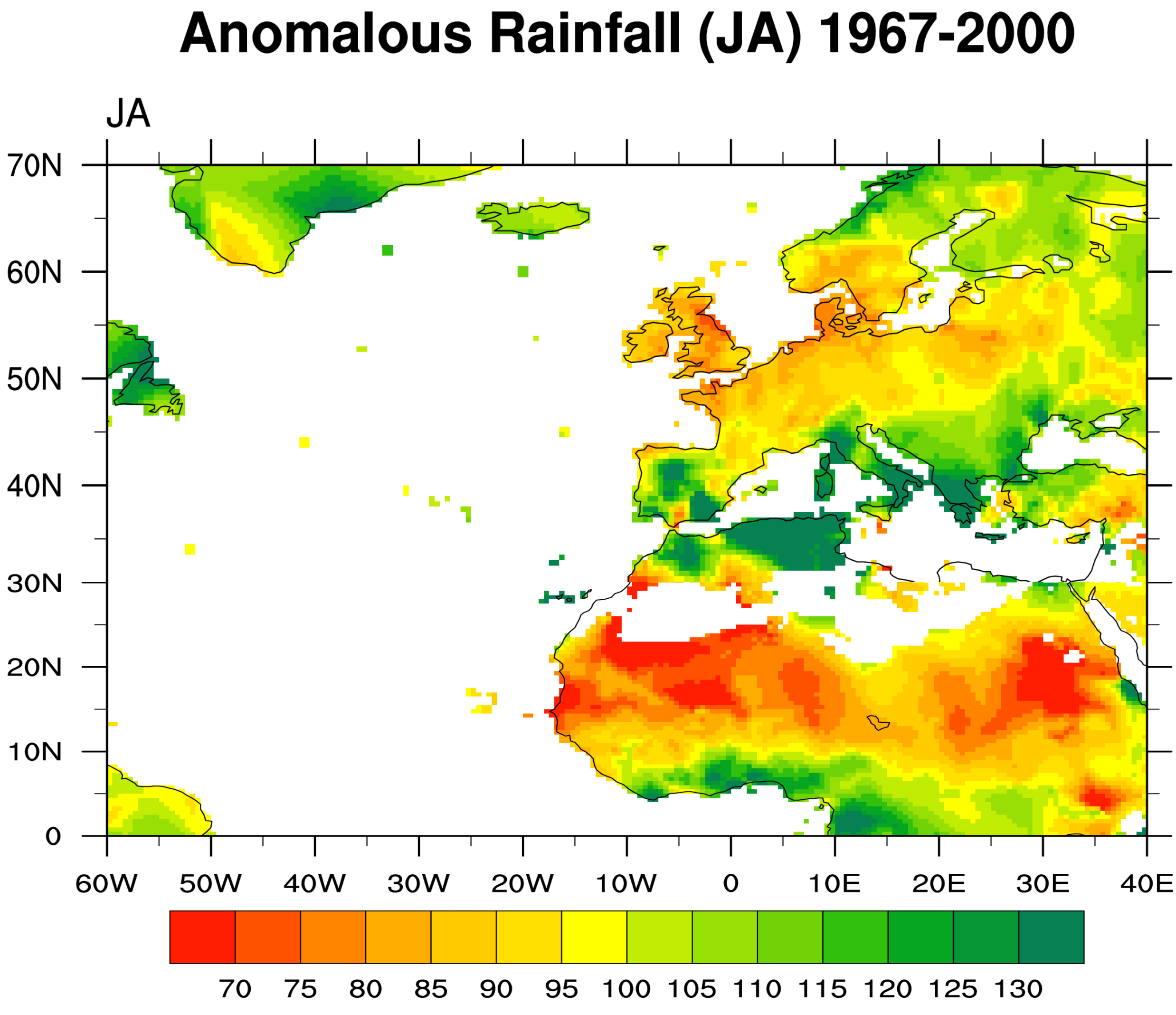

Figure 11d. Rainfall in 1967-2000 expressed as a percentage of that in 1921-60 for Europe and North Africa.

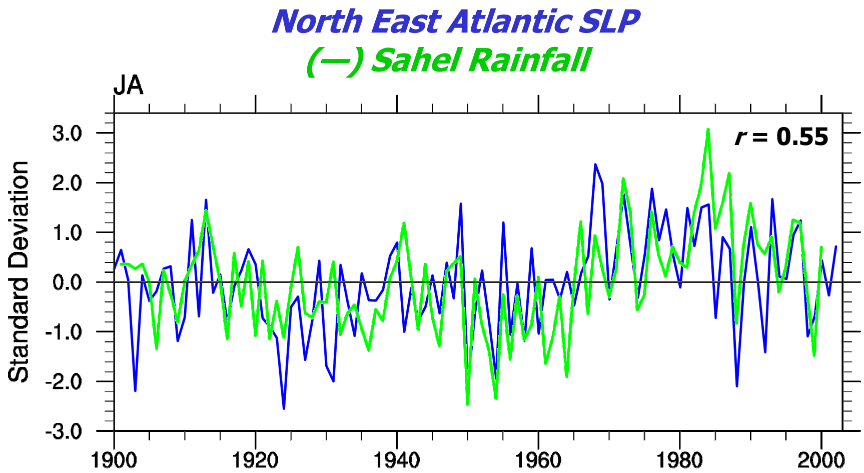

Figure 12. Summer Sahel rainfall (c.f. Nicholson 1985) and the mean sea level pressure in (approximately) the southern node of the high summer NAO (30°W-30°E, 40°N-70°N) as indicated by EOF1, 1899-2002.

It is well known that sea surface temperature in various parts of the world has an influence on Sahel rainfall (e.g. Folland et al, 1986, Rowell et al, 1995), partly through modulation of the moisture flux convergence into, and latitude of, the North African Intertropical Convergence Zone (Rowell et al, 1992). Indeed SST is used as the main factor in UK Met Office seasonal forecasts of North African rainfall (Folland et al, 1991). On the decadal time scale, SST influences are very widespread as shown by individual ocean basin SST experiments with a climate model described in Folland et al (1991). Thus could variations in the high summer NAO be physically linked to variations in the West African summer monsoon?

To investigate any SST links with the summer NAO, we look first at variations of SST on subdecadal time scales (Fig 13). SST is taken from the HadISST data set (Rayner et al, 2003) using the period 1870-2003. Figs 13c, 13d show some apparent influence of ENSO on the high summer NAO in the lead SST field (June and July mean), which strengthens as the season progresses. There appears to be some influence of a tripole pattern of SST in the North Atlantic in the lead SST pattern as well, though this disintegrates to a near monopole as the season progresses. Credibility is added to these results by comparison of the left and right SST diagrams. The two NAO clusters are taken from independent days but as might be hoped, the SST anomaly patterns are largely opposite in sign. However no other region than the two described above clearly has an influence – thus elsewhere there is lack of persistence in SST when going from the lead SST pictures (Figs 13c, 13d) to the lag SST (August and September, Figs 13g,13h). The large SST anomalies that develop near the UK during and after the summer NAO period are very likely to be a local response to anomalous cyclonic (cold SST) or anticyclonic forcing (warm SST) from the summer NAO itself and it remains to be discovered which are the real influencing regions for this important mode of summer climate variability. Note that an ENSO link is also seen with Sahel rainfall (Folland et al, 1991). However any link to the summer NAO needs careful study.

Time has not allowed the exploration of decadal to multidecadal links with SST. These will follow in a future report, but based on work with Sahel rainfall, these are expected given the similarity of the time series in Fig.12.

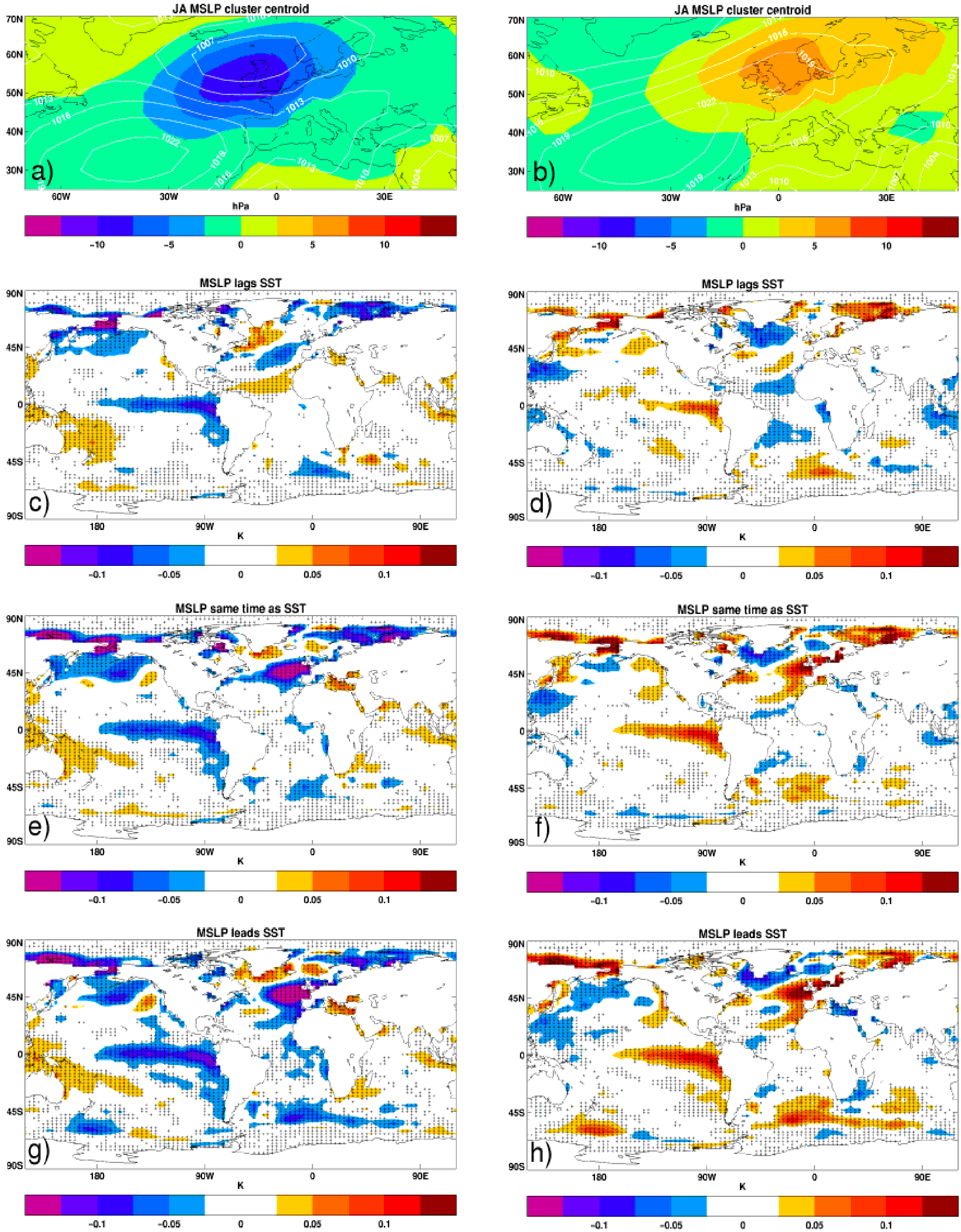

Figure 13. Association between the two summer NAO clusters and SST worldwide, filtered to accept only interannual variations of SST. Below each EMSLP cluster centroid (a,b) are displayed the associated SST anomalies where SST leads MSLP (c,d), SST and MSLP are simultaneous (e,f) and SST lags MSLP (g,h).

4) Possible links between the El Niño Southern Oscillation (ENSO) and European climate.

Although ENSO is perhaps the most prominent natural mode of variability in tropospheric climate, robust European effects of ENSO have so far been difficult to ascertain. In particular, despite some claims of reproducible effects of ENSO in individual events (e.g. Dong et al. 2000, Brönnimann et al. 2004) there has been little consensus on the remote response to ENSO over Europe. Indeed, it has been recently shown (Greatbatch et al. 2004) that the response to ENSO over Europe varies in sign with the temporal period chosen for analysis and may therefore be non-stationary. Here we suggest nonlinearity as an alternative explanation for the uncertainty in the European response to ENSO. This is illustrated in Figures 14-15 which show 200hPa eddy geopotential height and MSLP anomalies from composites of weak and strong ENSO events in Jan-March. In the weak ENSO case (upper panels in Figure 14), there is a statistically significant response in the upper level height over the tropical Pacific with a wavetrain extending out to higher latitudes across the Pacific basin. However, the response over the North Atlantic and Europe is weak and generally not statistically significant.

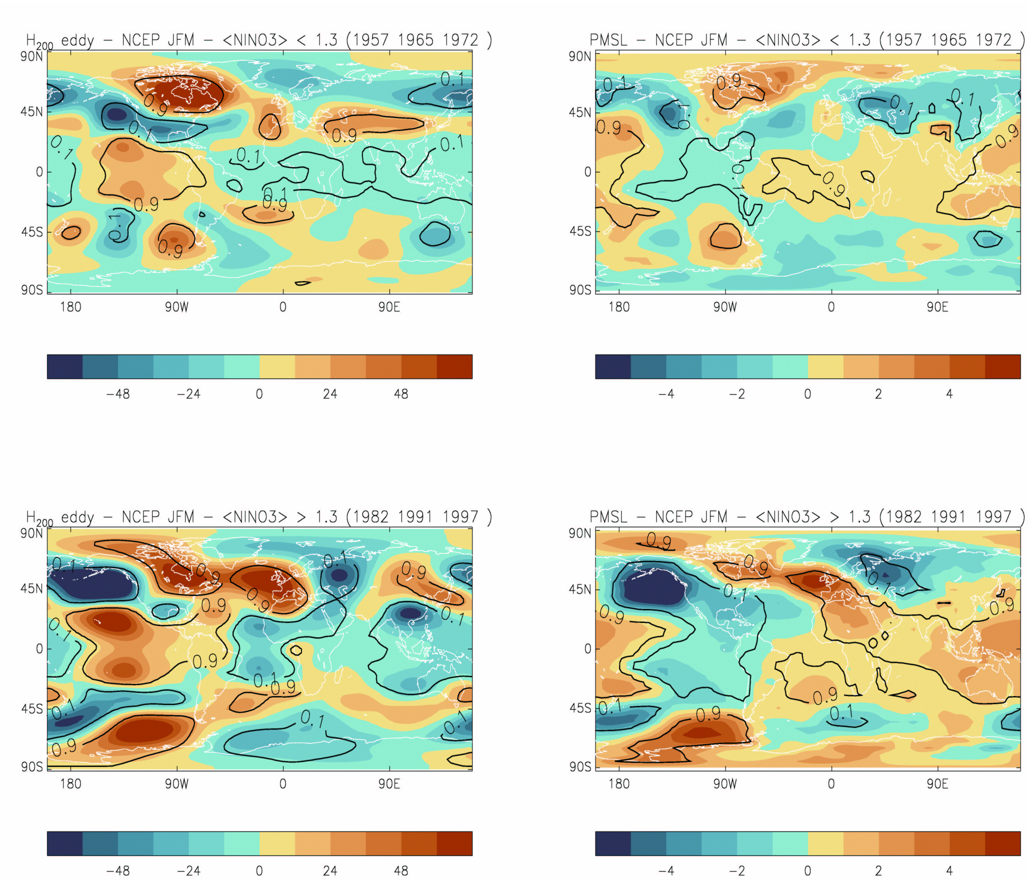

Figure 14. Composite ENSO anomalies for weak events (upper) and strong events (lower) over the latter half of the 20th Century. Eddy geopotential heights at 200hPa (left) and mean sea level pressure (right) are plotted in units of m and hPa respectively from NCEP data (Kalnay et al. 1996). 90% significance levels from a t-test are shown by black contours. Composites are based on the NINO3 index derived from HadISST. Anomalies are calculated with respect to 20-year running-window climatological means.

For large-amplitude ENSO events (see lower panels) there is also a secondary effect of reduced geopotential height over the tropical Atlantic, with an eddy anomaly of similar pattern but opposite sign to the Pacific anomaly suggesting reduced tropospheric heating. The stronger positive height anomaly over the tropical Atlantic region and the midlatitude European region may be part of a second wavetrain which

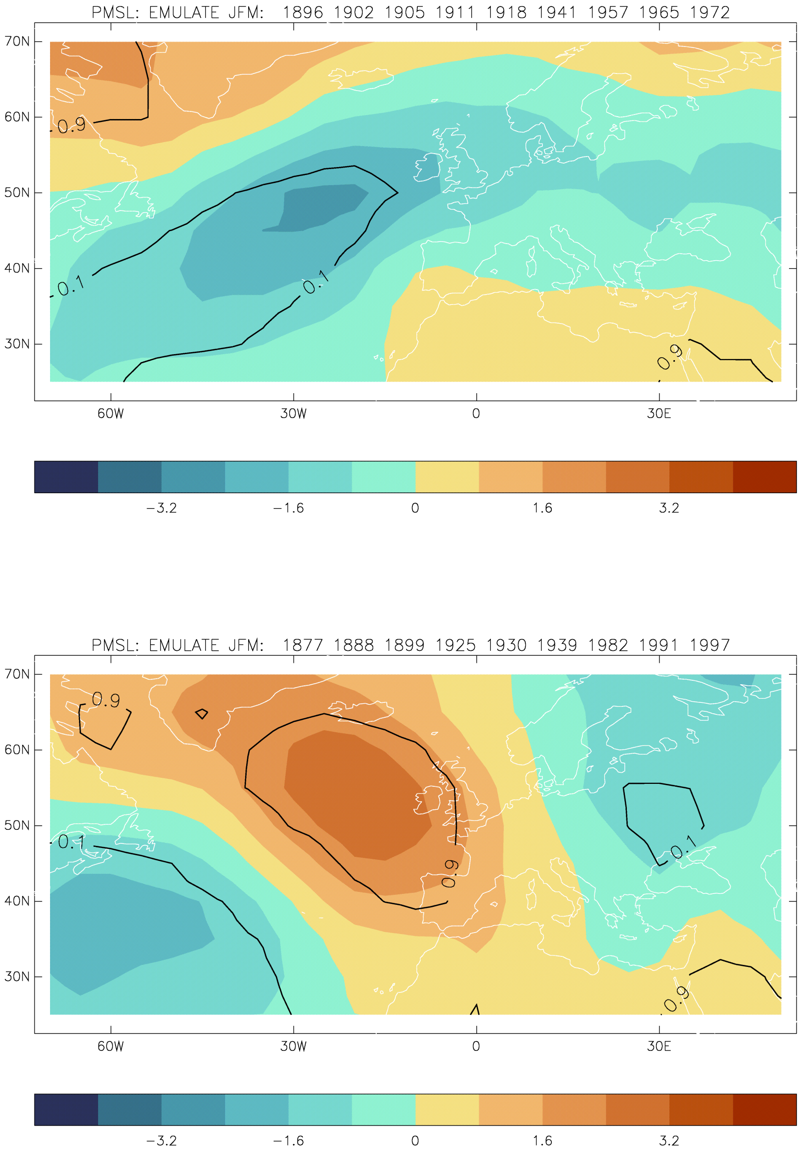

Figure 15. Composite ENSO anomalies in Jan-March for weak events (upper) and strong events (lower) over the period 1850-2000. Data are from the new EMULATE dataset of mean sea level pressure and are plotted in units of hPa. 90 % significance levels from a t-test are shown by black contours. Anomalies are calculated in the same way as for the NCEP data.

emanates from this region. The sea level pressure anomalies show in all cases a largely barotropic ENSO-signal over Western Europe which however becomes a statistically significant dipolar surface pressure anomaly (oriented SW-NE) only in the strong ENSO case.

The suggestion of a possible non-linear effect on European climate in mid to late winter is supported by the EMULATE surface pressure dataset which extends further into the past. Figure 15 shows similar composites of weak and strong ENSO events which include all warm events since 1870. The extended set of strong ENSO events captured here show a similar pattern to the analysis limited to the latter part of the 20th century using NCEP data. The weak events also show a similar pattern to the smaller sample in the NCEP data but the negative anomaly over the Pacific is now statistically significant and extends further eastwards.

5) Conclusions

We have shown significant links between SST and the frequency of daily weather patterns as well as seasonally averaged atmospheric anomaly patterns. In particular, the winter NAO and summer NAO show links with a tripole like pattern of North Atlantic SST and there is likely to be some predictability in the frequency of winter NAO-like weather regimes from spring SST as previously shown explicitly by Rodwell and Folland (2003). Both temperature across Europe and European precipitation also show strong links with the NAO and tripolar Atlantic SST anomalies, with Northern Europe being wetter and Southern Europe being drier during periods of positive NAO.

The summer NAO appears to be a robust phenomenon, appearing in a similar way in EOF and cluster analyses of sea level pressure. It is a dipolar anomaly in surface pressure that corresponds to a large change over NW Europe relative to the variability. Its pattern is such that it has maximum influence in high summer near locations where its southern node varies from cyclonic to anticyclonic. This coincides closely with UK and coastal North West Europe. It exhibits a similar spectrum of variations to the winter NAO but these are essentially uncorrelated. We have concentrated on rainfall influences in this note as the tendency to droughts and floods is probably the most important impact of the summer NAO. Nevertheless, temperature influences will also be important and need investigation. Like the winter NAO, interannual variations in the summer NAO may also be forced by a tripolar SST pattern. Unlike the winter pattern, its feedback on the ocean appears to be a more uniform change in East Atlantic SST: with warming in positive summer NAO (anticyclonic) conditions and cooling in negative summer NAO (cyclonic) conditions. There also appears to be an association of the summer NAO with the North African monsoon throughout the twentieth century, but the mechanism of this, if it exists, requires model studies. The influences of SST on decadal time scales also need investigation.

Because of its prominent role in climate variability we also examined the possible influence of ENSO on the European region. Extended analysis using the EMULATE sea level pressure data indicates a robust response over Europe in January to March in high amplitude ENSO events which could also lead to predictability in that season. The tropical Atlantic appears to play a role in this effect but again this requires model studies for verification.

This report represents a summary of the prominent areas of observational SST-atmosphere links being examined in the EMULATE project. Along with further decadal influences of SST on European climate currently being analysed, it will be used to guide modelling studies, and particularly SST perturbation experiments in the coming year.

References

Alexander, L.V. and P.D. Jones, 2001: Updated precipitation series for the U.K. and discussion of recent extremes. *Atmos. Sci. Letts* doi:10.1006/asle.2001.0025.

Brönnimann, S., Luterbacher, J., Staehelin, J., Svendby, T.M., Hansen, G., and Svenøe, T., 2004: Extreme climate of the global troposphere and stratosphere in 1940-42 related to El Niño, *Nature,* **431**, 971-974

Dong, B.W., Sutton R.T., Jewson S.P., O'Neill A. and Slingo J.M. 2000: Predictable Winter Climate in the North Atlantic Sector During the 1997-1999 ENSO cycle. Geophys Res. Lett., **27** (7), 985-988.

Folland, C.K., Parker, D.E. and T.N. Palmer, 1986: Sahel rainfall and worldwide sea temperatures 1901-85. *Nature*, **320**, 602-607.

Folland, C.K., Parker, D.E., Ward, M.N. and A. Colman, 1988: Sahel rainfall, N Hemisphere circulation anomalies and worldwide sea temperature changes. Study Week on "Persistent meteo-oceanographic anomalies and teleconnections", Pontifical Academy of Sciences, Rome, 23-27 Sept 1986, Ed: C. Chagas and G. Puppi. *Pontificiae Academiae Scientiarum Scripta Varia*, **69**, pp393-436.
Folland, C.K., Owen, J., Ward, M.N. and A. Colman, 1991: Prediction of seasonal rainfall in the Sahel region using empirical and dynamical methods. *J. Forecasting*, **10**, 21-56.

Frankignoul, C., 1985: Sea-Surface Temperature Anomalies, Planetary Waves and Air-Sea Feedback in the Middle-Latitudes, *Rev. Geophys.,* **23** (4), 357-390.

Greatbatch R.J., Lu J., Peterson A.K., 2004: Nonstationary impact of ENSO on Euro-Atlantic winter climate, Geophys. Res. Lett., **31**, doi:10.1029/2003GL018542.

Hurrell, J.W. and Folland C.K., 2002: The relationship between tropical Atlantic rainfall and the summer circulation over the North Atlantic. *CLIVAR Exchanges,* **25**, 52-54.

Hurrell, J. W., Kushnir, Y., Ottersen G. and M Visbeck, 2003: An overview of the North Atlantic Oscillation. In: The North Atlantic Oscillation - climatic significance and environmental impact. Eds Hurrell, J.W., Kushnir, Y., Ottersen, G. and M Visbeck, pp 1-35. Geophysical Monograph 134, American Geophysical Union, Washington, DC, pp279.

Kalnay E. et al. 1996: The NCEP/NCAR 40y Re-analysis Project, *Bull. Amer. Met. Soc.,* **77** (3), 437-471.

Michelangeli P.A., Vautard R., Legras B., 1995: Weather Regimes - Recurrence and Quasi Stationarity, *J. Atm. Sci*, **52** (8): 1237-1256.

Nicholson S.E., 1985: Sub-Saharan rainfall 1901-1984, *J. Clim. Appl. Meteorol.,* **24**, 1388-1391.

Rayner, N.A., Parker, D.E., Horton, E.B., Folland, C.K., Alexander, L.V., Rowell, D.P., Kent, E.C., and A. Kaplan, 2003: Global analyses of sea surface temperature, sea ice, and night marine air temperature since the late nineteenth century. *J. Geophys. Res*., **108(**D14), 4407, doi: 10.1209/2002JD002670, 2003. (29pp + 8 supplementary colour pages).

Rodwell, M., Rowell, D.P. and C.K. Folland, 1999: Oceanic forcing of the wintertime North Atlantic Oscillation and European climate. *Nature*, **398**, 320-323.

Rodwell, M.R. and C.K. Folland, 2002: Atlantic air-sea interaction and seasonal predictability, *Q. J. Roy. Met. Soc.*, **128**(583):1413-1443.

Rodwell, M.R. and C.K. Folland, 2003: Atlantic air-sea interaction and model validation. *Annals of Geophysics. Special Issue for results of EU SINTEX,* **46**, 47-56.

Rowell, D.P., Folland C.K., Maskell K. and M.N. Ward, 1995: Variability of summer rainfall over tropical North Africa 1906-1992, Observations and modelling. *Q.J.R. Met. Soc.*, **121**, 669-704.

Rowell, D.P., Folland, C.K., Maskell, K. and J.A. Owen, 1992: Modelling the influence of global sea surface temperature on the variability and predictability of seasonal Sahel rainfall. *Geophys. Res. Lett.*, **19**, 905-908.

Trenberth, K.E. and D.A. Paolino, 1980: Characteristic patterns of variability of sea level pressure in the Northern Hemisphere. *Mon. Weath. Rev.*, **108**, 855-872.

Acknowledgements:

Thanks to Jim Hurrell, NCAR, Boulder, Colorado for input on the summer north Atlantic Oscillation.